FEMS Microbiology Letters, 362, 2015, fnv006

doi: 10.1093/femsle/fnv006
Advance Access Publication Date: 19 January 2015
Research Letter

RESEARCH LETTER – Pathogens & Pathogenicity

msaABCR operon positively regulates biofilm development by repressing proteases and autolysis in *Staphylococcus aureus*

Gyan S. Sahukhal, Justin L. Batte and Mohamed O. Elasri*

Department of Biological Sciences, The University of Southern Mississippi, Hattiesburg, MS 39406-0001, USA

*Corresponding author: Department of Biological Sciences, The University of Southern Mississippi, Hattiesburg, MS 39406-0001, USA. Tel: +601-266-6916; E-mail: mohamed.elasri@usm.edu

One sentence summary: *msaABCR* regulates proteases, cell death and biofilm formation in *Staphylococcus aureus*.

Editor: Akio Nakane

ABSTRACT

Staphylococcus aureus is an important human pathogen that causes nosocomial and community-acquired infections. One of the most important aspects of staphylococcal infections is biofilm development within the host, which renders the bacterium resistant to the host's immune response and antimicrobial agents. Biofilm development is very complex and involves several regulators that ensure cell survival on surfaces within the extracellular polymeric matrix. Previously, we identified the *msaABCR* operon as an additional positive regulator of biofilm formation. In this study, we define the regulatory pathway by which *msaABCR* controls biofilm formation. We demonstrate that the *msaABCR* operon is a negative regulator of proteases. The control of protease production mediates the processing of the major autolysin, Atl, and thus regulates the rate of autolysis. In the absence of the *msaABCR* operon, Atl is processed by proteases at a high rate, leading to increased cell death and a defect in biofilm maturation. We conclude that the *msaABCR* operon plays a key role in maintaining the balance between autolysis and growth within the staphylococcal biofilm.

Key words: *Staphylococcus aureus*; proteases; *msaABCR*; regulation; biofilm; autolysis

INTRODUCTION

Staphylococcus aureus is a Gram-positive human pathogen that causes nosocomial and community-acquired infections. The increasing prevalence of antibiotic resistance and production of biofilm by *S. aureus* makes these infections difficult to treat. Indeed, biofilm formation is responsible for the establishment of chronic infections such as osteomyelitis, infective endocarditis, indwelling-medical-device-associated infections and chronic wound infections (Herold *et al.*, 1998; Lowy 1998; Haque *et al.*, 2007). The molecular mechanism of biofilm formation and the associated global regulatory network are still poorly understood. *Staphylococcus aureus* produces a very well-organized, multilayered, 3D mushroom-shaped biofilm embedded in an extracellular polymeric matrix composed of poly-*N*-acetylglucosamine (PIA), extracellular DNA (eDNA) and several heterogeneous proteins (Cramton *et al.*, 1999; Whitchurch *et al.*, 2002; Rice *et al.*, 2007; Merino *et al.*, 2009; Houston *et al.*, 2011).

Several studies have determined the genes involved in regulating biofilm development. Transcriptional regulators, including stress response sigma factor B (*sigB*), staphylococcal accessory regulator A (*sarA*), the two-component system *arlRS* and the accessory gene regulator (*agr*), have been shown to play key roles in the regulation of biofilm development (Kullik, Giachino and Fuchs 1998; Beenken, Blevins and Smeltzer 2003; Boles and Horswill 2008; Tsang *et al.*, 2008). Several operons like *icaADBC*, *dltABCD*, *cidABC* and *psmβ* operons also regulate biofilm formation (Heilmann *et al.*, 1996; Gross *et al.*, 2001; Rice *et al.*, 2007; Otto 2013). Other factors, such as secreted proteases, eDNA, major

Received: 8 December 2014; **Accepted:** 12 January 2015

autolysin (Atl) and nucleases, also play major roles in the maintenance and dispersion of biofilms (Qin *et al.*, 2007; Rice *et al.*, 2007; Houston *et al.*, 2011; Kiedrowski *et al.*, 2011; Beenken *et al.*, 2012; Chen *et al.*, 2013).

Despite our current knowledge of the many regulators and factors involved in biofilm development, there is still no consensus on the regulation of biofilm development among the diverse staphylococcal strains nor on the strain-dependent regulation of biofilm development. For instance, several studies have shown that different *Staphylococcus* strains regulate biofilm formation using various mechanisms such as PIA-dependent, PIA-independent and eDNA-dependent mechanisms (Cramton *et al.*, 1999; Whitchurch *et al.*, 2002; Fitzpatrick, Humphreys and O'Gara 2005; Toledo-Arana *et al.*, 2005; Rice *et al.*, 2007; Mann *et al.*, 2009).

We previously identified a new operon, *msaABCR*, which includes two non-coding RNAs, *msaC* and the antisense RNA, *msaR*, which are essential for the regulation of the *msaABCR* operon. The *msaABCR* operon regulates important phenotypes in *S. aureus*, including biofilm development and virulence (Sahukhal and Elasri 2014). The *msaABCR* operon also regulates the expression of key global regulators *sarA, agr* and *sigB* (Sahukhal and Elasri 2014). The regulatory mechanism of the *msaABCR* operon is not yet defined. In this study, we show that the *msaABCR* operon regulates biofilm development by controlling the rate of autolysis. We also show that this operon controls cell death by regulating the rate of processing of the major autolysin Atl by proteases.

METHODS

Bacteria and growth conditions

In this study, we used *S. aureus* strains USA300˙LAC and RN4220 and the *Escherichia coli* strain, DH5α. The *S. aureus* strains were grown in tryptic soy broth (TSB) or tryptic soy agar, as appropriate. The *E. coli* strain was grown in Luria–Bertani broth. Antibiotics (chloramphenicol, 10 μg ml^{-1}; erythromycin, 10 μg ml^{-1} and ampicillin, 100 μg ml^{-1}) were used as necessary. The strains and plasmid constructs used in this study are listed in Table 1.

Construction of double-deletion mutants

We used a previously described mutagenesis protocol (Bae and Schneewind 2006; Sahukhal and Elasri 2014) to construct a non-polar, in-frame double-deletion mutant *msaABCR/atl* and LAC *msaABCR*/protease. Deletions were verified by end-point and real-time quantitative PCR (qPCR), as described previously (Sahukhal and Elasri 2014).

Biofilm assays

A microtiter biofilm assay was performed as described previously (Sambanthamoorthy *et al.*, 2008; Sahukhal and Elasri 2014). To study the effect of polyanethole sulfonate (PAS) treatment on biofilm formation, the biofilm was grown in biofilm medium in the presence of 500 μg ml^{-1} PAS, as previously described (Rice *et al.*, 2007). The mean values of three independent experiments, each performed in triplicate, are reported.

Confocal microscopic analysis of the biofilm

Biofilms were grown in 96-well Corning high content imaging microplates, as described previously (Sambanthamoorthy *et al.*, 2008; Sahukhal and Elasri 2014). The biofilm was grown for 48 h with shaking at 150 rpm. Each adherent biofilm was washed three times with sterile phosphate-buffered saline (PBS) and stained with 50 μl of live/dead stain [Syto-9 (1.3 μm) and Toto-3 (2.0 μm)] prepared in PBS, as previously described (Mann *et al.*, 2009). Images of the biofilms were acquired using confocal laser scanning microscopy (Zeiss 510 Meta CLSM) under a 40 × 1.4 oil DIC objective. The Syto-9 stain was excited with an argon laser at 488 nm and the emission band-pass filter used for Syto-9 was 515 ± 15 nm. The Toto-3 stain was excited with an HeNe laser at 633 nm, and emissions were detected with a 680 ± 30 nm filter. Z-stacks were collected at 1.0 μm intervals. Images were processed with the COMSTAT software to quantify the total biomass, biofilm thickness, number of dead cells and amount of eDNA (Heydorn *et al.*, 2000).

Autolysis assay

Autolysis assays were performed as described previously (Mani, Tobin and Jayaswal 1993). To study the effect of PAS on autolysis, the cultures of *S. aureus* were diluted to an OD_{600} of 0.05 in TSB containing 1 M NaCl and 500 μg ml^{-1} of PAS and allowed to grow at 37 °C with shaking until an OD_{600} of 0.7 was reached. The cells were harvested and the autolysis assay was performed in 0.05 M Tris-Cl (pH 7.2) containing 0.025% Triton X-100. The absorbance (OD_{580}) was measured every 30 min to quantify cell lysis. All the experiments were repeated three times and statistical significance tests (paired *t*-tests) were performed using the GraphPad software.

Zymographic analysis

Zymographic analyses of the cell-wall-bound and extracellular fractions of murein hydrolases were performed as described previously (Mani, Tobin and Jayaswal 1993). Freeze–thaw extracts, also designated 'cell-wall-bound autolysins', were isolated from cells grown to mid exponential phase, as described previously (Mani, Tobin and Jayaswal 1993; Ledala, Wilkinson and Jayaswal 2006). The extracellular autolysins Atl were isolated by the centrifugation of whole-cell cultures grown to late exponential phase. The supernatant was collected and used for zymographic analysis. The enzyme extracts were concentrated using Amicon Ultracel (3K) centrifugal filters. The proteins were quantified with Quick Start™ Bradford reagent.

The zymographic analysis was performed with a 10% polyacrylamide-SDS gel containing 0.2% (wt/vol) crude cell walls from *S. aureus* (RN4220) or *Micrococcus luteus* (Bose *et al.*, 2012). The enzyme extracts (3 μg) were mixed with loading buffer and heated for 3 min in a boiling water bath before electrophoresis. After electrophoresis, the gel was washed twice with water and incubated overnight at 37°C in renaturation buffer (25 mM Tris-HCl [pH 8.0], 1% Triton X-100). Lytic activities were observed as clear bands in the opaque gel. The gels were stained with 1% methylene blue in 0.01% KOH before imaging.

Tolerance to lysostaphin, mutanolysin and lysozyme

Overnight-grown cells were diluted to an OD_{600} of 0.05 in TSB and allowed to grow at 37°C with shaking to an OD_{600} of 0.7. The cells were harvested, washed twice with ice-cold water and then resuspended in the same volume of 0.05 M Tris-Cl (pH 7.2) containing 2 μg ml^{-1} lysostaphin, 10 U ml^{-1} mutanolysin or

Table 1. Strains and plasmids used in this study

Strains or plasmids	Relevant characteristics	Source
Plasmids		
pKOR1	*E. coli*– *S. aureus* shuttle vector, ori(Ts) inducible, secY antisense counterselection, Amp^r Cm^r	Dr Bae
pMOE 399	pKOR1: Δ *msa* operon deletion construct	This study
pCN34	pT181-based low copy number *E. coli*–Staphylococcal shuttle vector	NARSA
pMOE 403	pCN34-*msaABCR* operon :: *msaABCR* operon complement	This study
pCN58	pT181-based *E.coli* –staphylococcal shuttle vector that contains promoterless LuxAB as a reporter gene for promoter-gene fusion.	NARSA
pMOE 481	pCN58-Promoter ^{aur}	This study
pMOE 482	pCN58-Promoter ^{ssp}	This study
pMOE 483	pCN58-Promoter ^{scp}	This study
pMOE 498	pCN58-Promoter ^{spl}	This study
pMOE 501	pCN58-Promoter	This study
pMOE 448	*E. coli* pCN51 vector with pCAD inducible promoter	This study
Strains		
RN4220	Restriction deficient mutant of 8325–4	NARSA
M. luteus	ATCC No. 4698	Sigma–Aldrich
LAC	CA-MRSA USA300 strains	Dr Shaw
MOE 401	LAC :: Δ *msaABCR* deletion mutant	This study
MOE 404	LAC 401 :: pMOE403 :: *msaABCR* complement into *msaABCR* deletion mutant	This study
	MOE 401/pCN34-vector control	This study
MOE 508	LAC 13C (Δ*atl*)	Dr Jeffrey Bose /K. Bayles
MOE 458	LAC/proteases	Dr Mark Smeltzer
MOE 512	*msaABCR*/*atl* mutant	This study
MOE 466	*msaABCR*/protease mutant	This study
	msaABCR complement into *msaABCR*/*atl* mutant	This study
MOE 467	*msaABCR* complement into *msaABCR*/protease mutant	This study
MOE 535	LAC :: Δ *sarA*:kan insertional mutant	This study
MOE 532	LAC :: Δ *msaABCR* deletion/*sarA*:kan insertional mutant	This study
MOE 533	*msaABCR*/*sarA*:kan mutant with pCN51-*sarA* vector	This study
MOE 536	*sarA*:kan mutant with pCN51-*sarA* vector	This study
MOE 545	*msaABCR* deletion mutant with pCN51-*sarA* vector	This study
MOE 645	LAC :: pCN58-Promoter ^{aur}	This study
MOE 646	LAC :: pCN58-Promoter ^{scp}	This study
MOE 647	LAC :: pCN58-Promoter ^{spl}	This study
MOE 648	LAC :: pCN58-Promoter ^{ssp}	This study
MOE 649	MOE 401 :: pCN58-Promoter ^{aur}	This study
MOE 650	MOE 401 :: pCN58-Promoter ^{scp}	This study
MOE 651	MOE 401 :: pCN58-Promoter^{spl}	This study
MOE 652	MOE 401 :: pCN58-Promoter^{ssp}	This study
MOE 495	LAC :: pCN58-vector control	This study

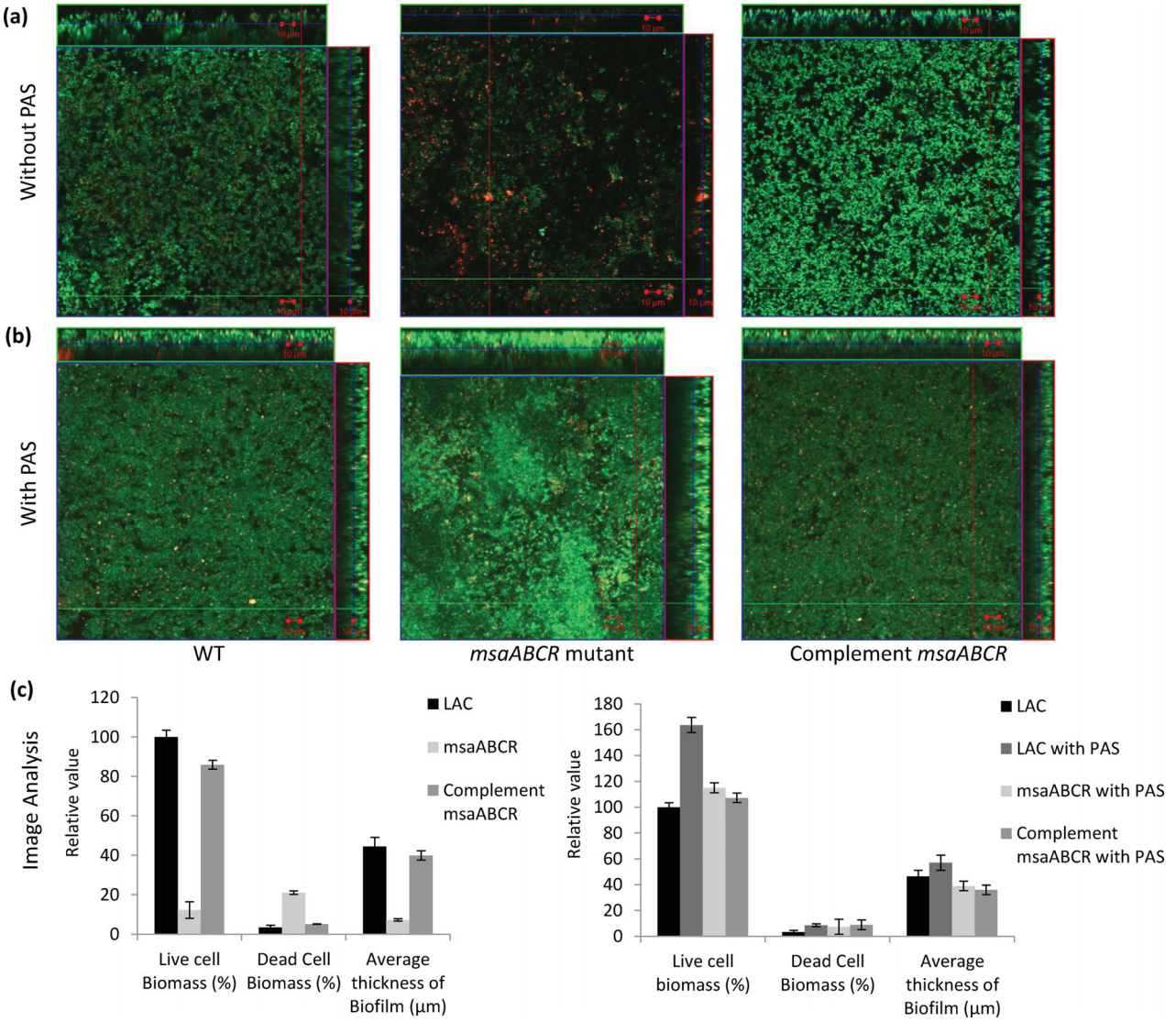

Figure 1. CLSM images and image analysis of the biofilm. Biofilm was grown upto 48 h and stained with Syto-9 (live cells, green) and Toto-3 (dead cells and eDNA, red). Panel **(a)** wild-type *S. aureus* USA300 LAC, *msaABCR* deletion mutant and *msaABCR* complement, respectively. Panel **(b)** CLSM image of biofilm of wild-type *S. aureus* USA300 LAC, *msaABCR* deletion mutant and *msaABCR* complement, respectively, grown in presence of 500 μg ml^{-1} PAS. Panel **(c)** COMSTAT image analysis of biofilm (a) and (b). These images are representative of three independent experiments. Scale bar represents 10 μm.

10 μg ml^{-1} lysozyme. The cells were incubated at 37°C with shaking and lysis was calculated from the OD_{600}.

RNA isolation and real-time qPCR

Total RNA for the RT-qPCR was isolated from cells using a Qiagen RNeasy Maxi column (Qiagen), and RT-qPCR was done as described previously (Sambanthamoorthy, Smeltzer and Elasri 2006). Analysis of expression of each gene was done based on at least three independent experiments. Two-fold or higher changes in gene expression were considered significant. All the primers used for RT-qPCR are listed in Table S1 (Supporting Information).

Construction of protease promoter–*luxAB* fusions and luciferase assays

The *E. coli*–staphylococcal shuttle vector pCN58 was used in this study to analyze transcriptional fusions (Charpentier *et al.*, 2004). The promoter regions of four different protease genes [aureolysin (*aur*), staphopain (*scp*), cysteine (*ssp*) and serine (*spl*)] were fused to *luxAB*, as previously described (Mootz *et al.*, 2013; Sahukhal and Elasri 2014). To study the promoter–luciferase activity, the bacterial cells (5 ml) were harvested at different optical densities (OD_{600} of 0.7, 1.5 and 4.0) representing the early, mid and late exponential growth phases, respectively. Promoter activity was also measured from 24, 48 and 72 h biofilms. Relative luminescence units were measured as described in (Sahukhal and Elasri 2014). The promoterless version of the reporter gene plasmid (pCN58) was used as a negative control.

RESULTS

Deletion of the *msaABCR* operon causes a defect in biofilm development

We have previously shown that the deletion of the *msaABCR* operon in *S. aureus* leads to a defect in biofilm formation

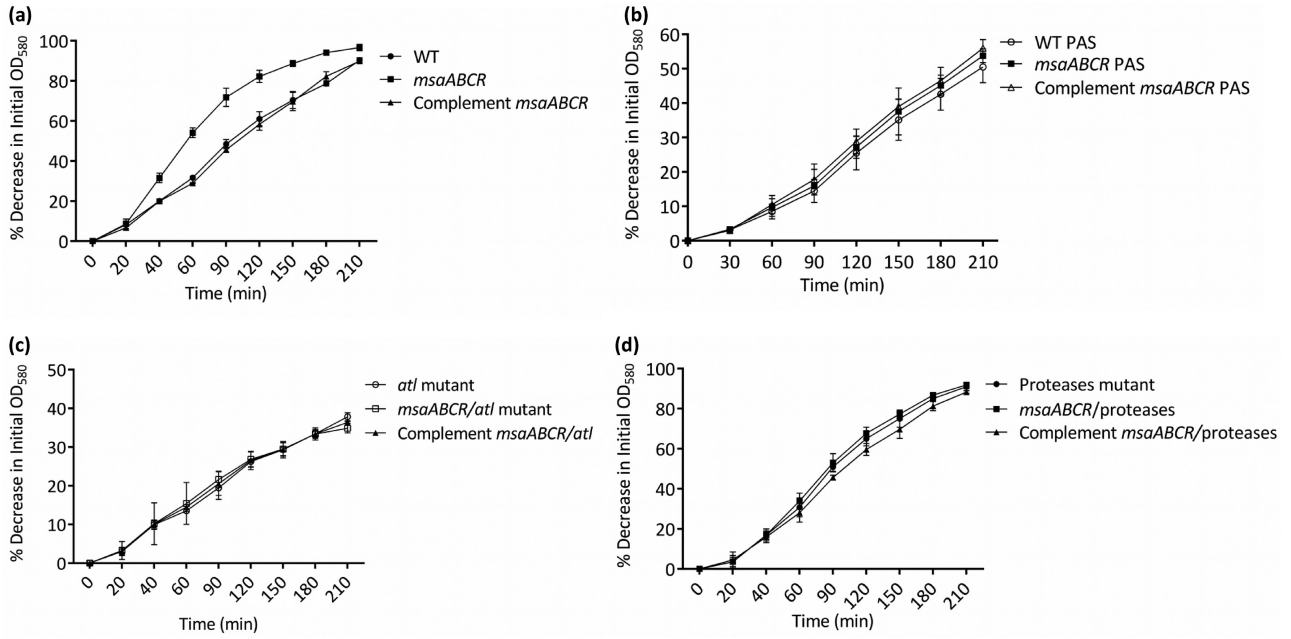

Figure 2. Triton-X-100-induced autolysis assay. **(a)** Rates of autolysis of wild-type *S. aureus* USA300 LAC, *msaABCR* deletion mutant and *msaABCR* complement. **(b)** Rate of autolysis measured in presence of 500 μg ml^{-1} PAS. Wild-type *S. aureus* USA300 LAC, *msaABCR* deletion mutant and *msaABCR* complement. **(c)** Rates of autolysis of *atl* mutant, *msaABCR/atl* double mutant and *msaABCR* complement in *msaABCR/atl* double mutant. **(d)** Rates of autolysis of *protease* mutant, *msaABCR/protease* double mutant and *msaABCR* complement in *msaABCR/protease* double mutant. The experiments were repeated at least three times. A paired *t*-test was used in the statistical analysis with the GraphPad software ($p < 0.0001$).

(Sahukhal and Elasri 2014). In this study, we investigated the mechanism behind this phenotype. We examined the biofilm formation of the *msaABCR* deletion mutant using confocal microscopy after staining with live/dead stain, Syto-9 and Toto-3. Syto-9 stains live cells green, whereas Toto-3 stains dead cells and eDNA red (Fig. 1a). We observed an increase in localized cell death within the biofilm of the deletion mutant relative to that of the wild-type or the complemented mutant. The mutant biofilm also lacked mature biofilm towers. We also analyzed the Z-stack confocal images with the COMSTAT image analysis software, and found that the biofilm of the *msaABCR* deletion mutant was relatively thin (7 μm, compared with 44 μm in the wild type) and dispersed, with a live cell biomass of only 12% compared with that of the wild-type biofilm, which was set to 100%. COMSTAT image analysis also showed the presence of more dead cells and eDNA in the *msaABCR* mutant biofilm (21%) relative to their levels in the wild-type biofilm (3%) (Fig. 1c). The complemented mutant showed a phenotype similar to the wild-type phenotype (Fig. 1a). These results suggest that the defective biofilm of the *msaABCR* mutant is attributable to an increased rate of cell death.

We confirmed these findings by measuring the rate of autolysis of the mutant during planktonic growth and found that in the presence of Triton X-100, the *msaABCR* mutant is lysed at a higher rate (20–25%) than is the wild-type or complemented mutant (Fig. 2a). The treatment of the strains with PAS, a cell lysis inhibitor, provided further support for the role of cell death in the *msaABCR* operon defect (Fig. 1b and Fig. 2b). These findings indicate that the *msaABCR* operon is involved in the regulation of autolysis, which might be responsible for the biofilm defect in this mutant.

Biofilm developmental defect in the *msaABCR* mutant is mediated by increased processing of the major autolysin, Atl

We examined the mechanism involved in the increased cell death in the *msaABCR* mutant. We tested the susceptibility of whole cell-wall fractions to lysostaphin, mutanolysin and lysozyme extracted from the *msaABCR* mutant. We found no significant difference between the *msaABCR* mutant and the wild type, suggesting that cell-wall perturbation is not responsible for the increased autolysis of the mutant. We also measured the expression of all known murein hydrolase genes (*atl*, *lytM*, *lytM*, *sle1*, *lytX*, *lytY* and *lytZ*), and regulators of autolysis, the *cidABC* and *lgrAB* operon genes. We found no significant change in the expression of these genes in the mutant relative to that in the wild type (Table S2, Supporting Information). These findings indicate that the role of the *msaABCR* operon in autolysis is not attributable to cell-wall perturbation or the regulation of genes known to control cell death.

We have previously shown that the deletion of *msaABCR* increases protease activity (Sahukhal and Elasri 2014). Other studies have shown that murein hydrolases (e.g. Atl) are targeted by proteases, which thus affect the rate of autolysis in *S. aureus* (Horsburgh *et al.*, 2002; Biswas *et al.*, 2006; Rice *et al.*, 2007; Lauderdale *et al.*, 2009). Because the *msaABCR* operon does not regulate the expression of murein hydrolase genes, we used zymography to investigate its role in the protease-mediated processing of the murein hydrolases. We measured the activity of the murein hydrolases (cell-wall-bound and extracellular fractions) using whole cells of *M. luteus* and *S. aureus* (RN4220) as substrates. *Micrococcus luteus* cells

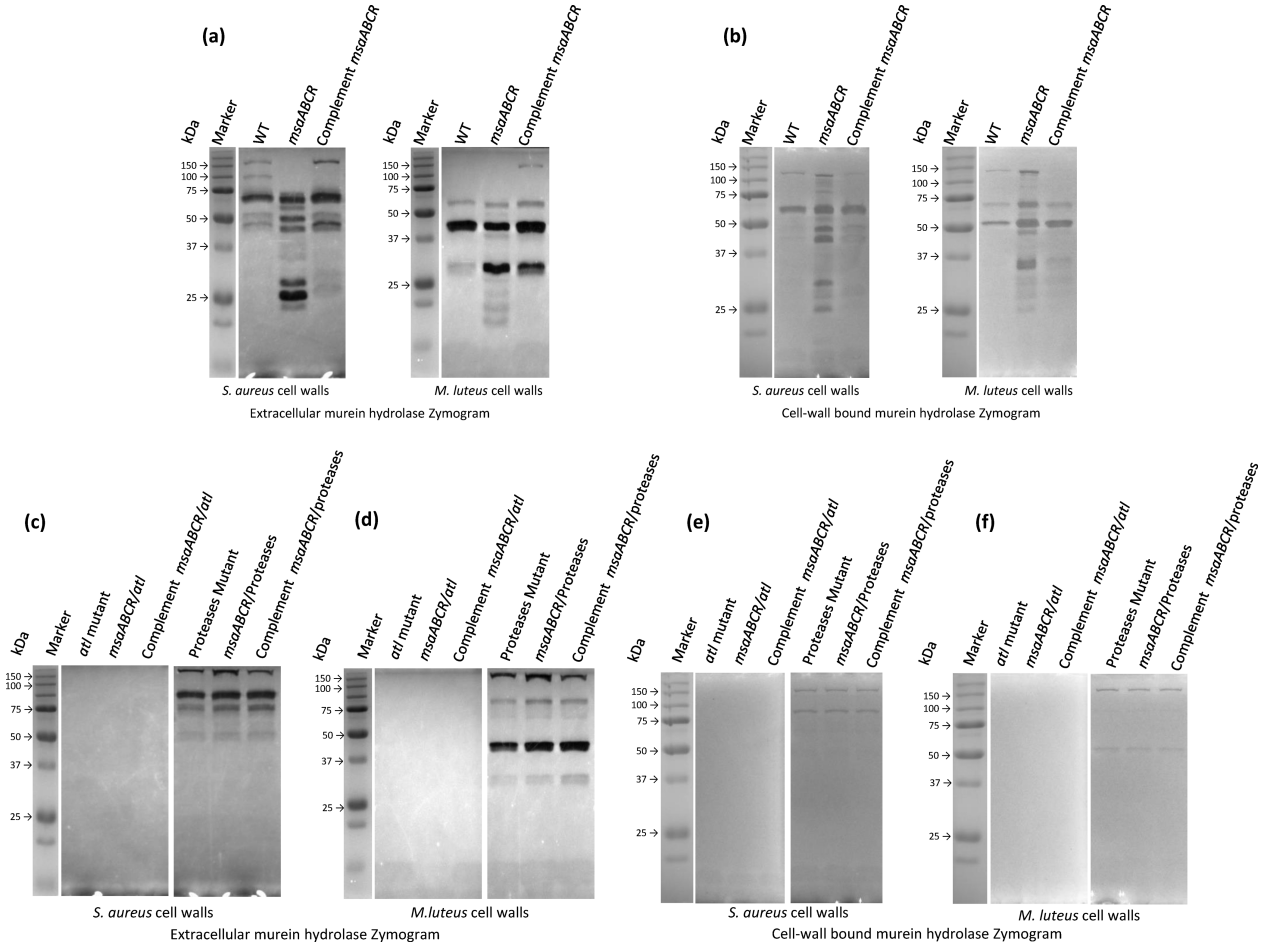

Figure 3. Extracellular and cell-wall bound murein hydrolase zymogram. *Staphylococcus aureus* cell wall and *M. luteus* cell-wall substrates were used in the zymogram to determine AM and GL classes of murein hydrolases. **(a)** Extracellular murein hydrolase zymogram of wild-type *S. aureus* USA300 LAC, *msaABCR* deletion mutant and *msaABCR* complement. **(b)** Cell-wall bound murein hydrolase zymogram of wild-type *S. aureus* USA300 LAC, *msaABCR* deletion mutant and *msaABCR* complement. **(c and d)** Extracellular murein hydrolase zymogram of *atl* mutant, *msaABCR/atl* double mutant, *msaABCR* complement in *msaABCR/atl* double mutant, *protease* mutant, *msaABCR/protease* double mutant and *msaABCR* complement in *msaABCR/protease* double mutant, respectively. **(e and f)** Cell-wall bound murein hydrolase zymogram of *atl* mutant, *msaABCR/atl* double mutant, *msaABCR* complement in *msaABCR/atl* double mutant, *protease* mutant, *msaABCR/protease* double mutant and *msaABCR* complement in *msaABCR/protease* double mutant, respectively.

and *S. aureus* cell-wall substrates were used to determine the various glucosaminidase (GL)-specific and amidase (AM)-specific activities, respectively, as previously described (Wadstrom and Hisatsune 1970; Oshida *et al.*, 1995; Bose *et al.*, 2012). The *msaABCR* deletion mutant showed a significantly altered pattern of AM and GL activities relative to those of the wild type and the complemented mutant (Fig. 3a and b). In the zymogram produced with *S. aureus* as the cell substrate, the *msaABCR* deletion mutant showed a significantly higher number of bands corresponding to AMs than the wild type in both the cell-wall-bound and extracellular fractions. When *M. luteus* cells were used as the substrate, we observed a similar pattern of activity for the GLs in both the cell-wall-bound and extracellular fractions (Fig. 3a and b).

Overall, the *msaABCR* mutant showed more processing of murein hydrolases, evident from the absence of high-molecular-weight bands and the presence of several additional low-molecular-weight bands in the zymogram relative to those in the wild-type zymogram (Fig. 3a and b).

The high-molecular-weight murein hydrolase bands correspond to the major autolysin (Atl) and its derivatives, whereas the low-molecular-weight murein hydrolase bands may have arisen from lytM, Sle1, LytN or LytH. Because we found no significant differences in the transcription levels of all known murein hydrolase genes between the wild type and the mutant, these findings suggest that the bands produced by the *msaABCR* mutant result from the increased processing of Atl. To investigate this possibility, we generated an *msaABCR/atl* double mutant. The double mutant showed increased production of extracellular proteases. However, this mutant showed no murein hydrolase activity in any of the fractions tested (Fig. 3c–f). The *msaABCR/atl* mutant also showed no increase in autolysis relative to that in the wild type (Fig. 2c). These findings support the conclusion that the observed murein hydrolase activity of the *msaABCR* mutant is primarily attributable to Atl processing.

To determine the contribution of proteases to this process, we fused the promoters of the genes (*aur*, *scp*, *ssp* and *spl*) encoding four major extracellular proteases to *luxAB* (Mootz *et al.*, 2013; Sahukhal and Elasri 2014). The luciferase assay of the *msaABCR* deletion mutant showed a significantly higher positive signal (production of light) relative to that produced by the wild type under all the growth conditions tested (early, mid and late exponential phases and biofilm) (Fig. 4). This confirms the role of

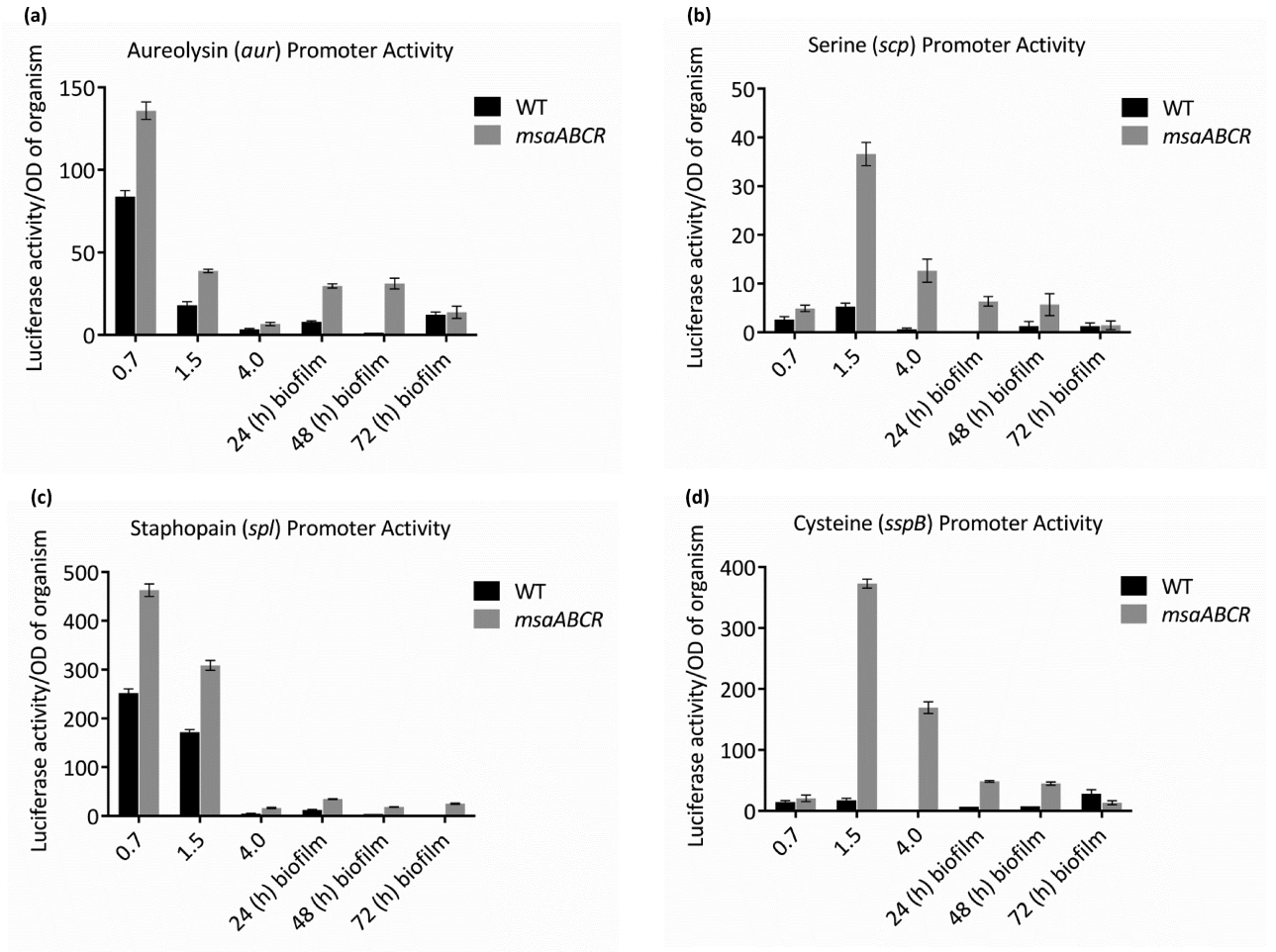

Figure 4. Promoter activities of protease genes. The activities of the protease promoters were measured in the wild-type and *msaABCR* deletion mutant. Luciferase activity (*luxAB*) was measured in three planktonic growth phases (early, mid and late exponential phases) and the biofilm. The vector pCN58 containing *luxAB* without a promoter was used as the negative control. **(a)** aureolysin (*aur*) promoter activity. **(b)** serine (*scp*) promoter activity. **(c)** staphopain (*spl*) promoter activity. **(d)** cysteine (*sspB*) promoter activity. The results are the means of three independent experiments, and each measurement was made in triplicate. Standard error bars are shown.

msaABCR in regulating the expression of the protease genes. We introduced the *msaABCR* deletion into an LAC protease knockout strain (Beenken *et al.*, 2010; Zielinska *et al.*, 2012) and measured its murein hydrolase activity, autolysis and biofilm formation. This mutant showed no evidence of high-molecular-weight murein hydrolase processing (Fig. 3c–f). Based on previous studies, the two bands produced by this mutant are presumed to correspond to Atl (Bose *et al.*, 2012; Grilo *et al.*, 2014). The *msaABCR*/protease mutant showed no increase in autolysis activity or any defect in biofilm formation (Figs 2d and 5). These results indicate that the *msaABCR* biofilm defect is mediated by the overproduction of proteases, which leads to the increased processing of murein hydrolases and increased cell death.

DISCUSSION

The *msaABCR* operon is essential for biofilm formation in *S. aureus* (Sahukhal and Elasri 2014). In this study, we set out to identify the mechanism underlying the regulatory role of *msaABCR* in biofilm formation. We have shown that the deletion of *msaABCR* results in the excessive production of proteases, leading to increased processing of the major autolysin, Atl. This in turn leads to uncontrolled cell death, which contributes to the biofilm defect in the *msaABCR* mutant. Controlled cell death and the controlled release of eDNA are important in the formation of a robust and mature biofilm in staphylococci and other organisms, including *Pseudomonas aeruginosa*, *Streptococcus intermedius*, *S. mutans* and *Enterococcus faecalis*. Many studies have shown that controlled cell death and the release of eDNA enhance biofilm formation, however, unregulated cell death may have detrimental effects on the biofilm (Wen, Baker and Burne 2006; Bayles 2007; Rice *et al.*, 2007; Boles *et al.*, 2010; Qamar and Golemi-Kotra 2012; Bitoun *et al.*, 2013; Chan *et al.*, 2013). Our findings are supported by several studies that have shown that excessive protease activity and autolysis results in biofilm instability and a lack of maturation, which reduces the growth rate within the biofilm and upsets the balance between its growth and detachment (Wen, Baker and Burne 2006; Boles *et al.*, 2010; Qamar and Golemi-Kotra 2012; Bitoun *et al.*, 2013; Chan *et al.*, 2013).

Several processes have been implicated in autolysis, including cell-wall perturbation, increased activity or expression of murein hydrolases, and the regulation of holin and antiholin expression (Perkins 1980; Wang *et al.*, 1992; Groicher *et al.*, 2000;

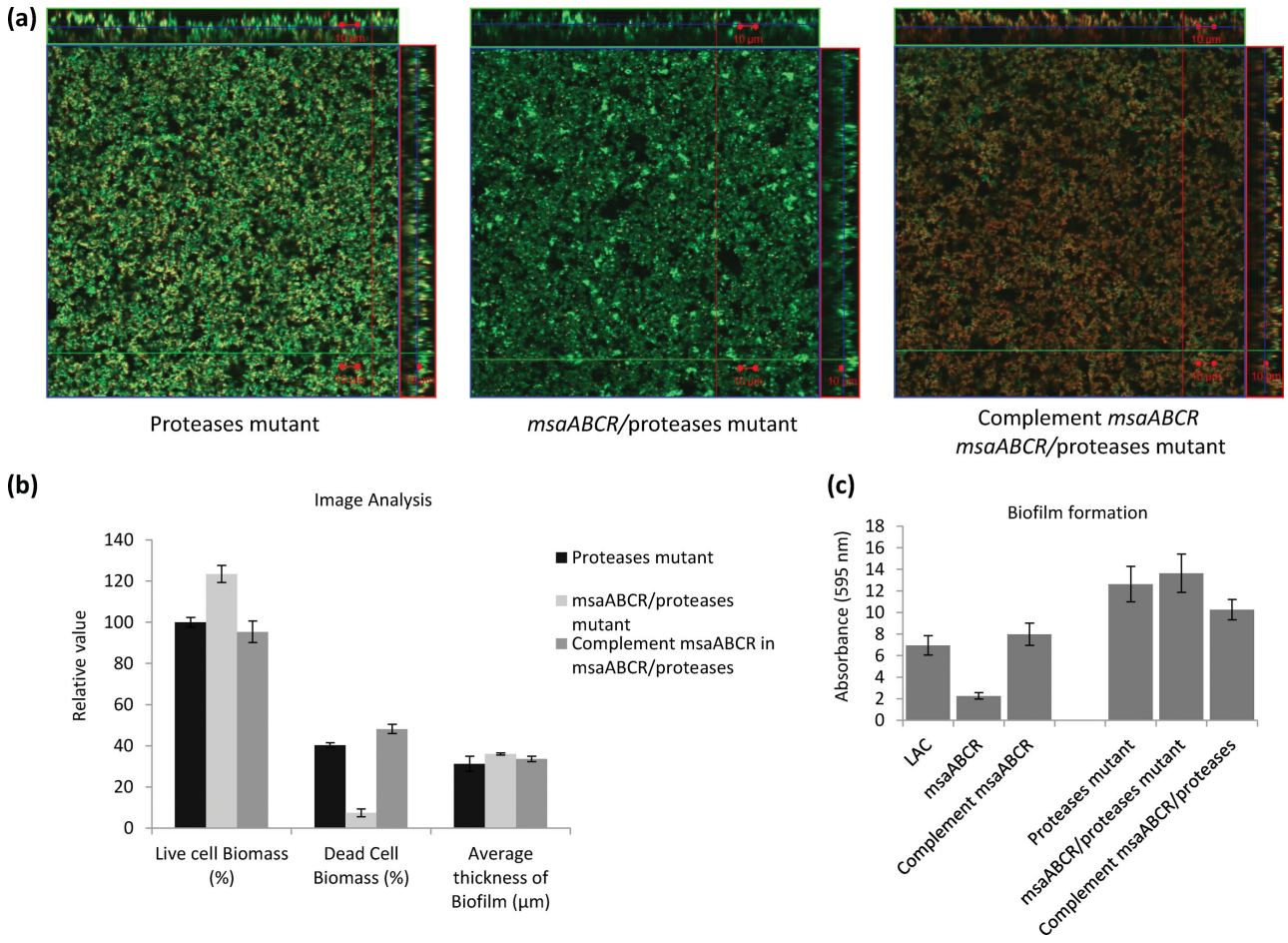

Figure 5. CLSM image and biofilm assay of *msaABCR*/protease double mutant. **(a)** CLSM images of protease mutant, *msaABCR*/protease double mutants and complement *msaABCR*/protease double mutants. **(b)** COMSTAT image analysis of CLSM images. **(c)** Microtiter biofilm assay of wild-types and double mutants. The results are representative of three independent experiments. Scale bar represents 10 μm.

Rice *et al.*, 2003; Bayles 2007; Qin *et al.*, 2007). The *msaABCR* operon regulates autolysis by controlling the processing of Atl by proteases. We found no evidence of the involvement of *msaABCR* in cell-wall perturbation or in regulating the expression of murein hydrolases, including Atl and the *cidABC*/*lrgAB* system. Previous studies have shown that Atl proprotein (134 kDa) contains an AM–GL peptide that is attached to a propeptide (Bose *et al.*, 2012; Grilo *et al.*, 2014). The proprotein is cleaved to yield a 117-kDa AM–GL peptide. This peptide is further processed to produce various AM intermediates (100, 81, 70 and 63 kDa) and GL intermediates. The GL intermediates include a 55-kDa peptide and two products that are slightly less than 55 kDa and lack the repeated domain. The 63-kDa Atl fragment corresponds to the mature AM band, with two repeat domains (AM-R1-R2), and the fragments slightly less than 63 kDa correspond to AM, with one repeat domain (AM-R1) and AM without any repeated domain. The high-molecular-weight bands of 134 and 117 kDa both showed AM and GL activity, whereas the lower-molecular-weight bands (100, 81, 70, 63, 48.75 and 30 kDa) showed AM-specific activity. The 55 kDa and other smaller bands (40.5 kDa and less) showed GM-specific activity. These patterns reflect the sequential order of Atl processing (Bose *et al.*, 2012; Grilo *et al.*, 2014). Our findings show that Atl is the main murein hydrolase regulated by *msaABCR*. Further support for this conclusion was obtained by examining the *msaABCR*/*atl* double mutant, which showed a complete lack of all the processing products described above (Fig. 3c–f).

We have previously shown that the *msaABCR* operon regulates protease production (Sahukhal and Elasri 2014). In this study, we linked the increase in proteases production to increased processing of Atl (Fig. 3c–f). We have shown that the *msaABCR* operon controls the expression of four extracellular proteases (Aur, Scp, Ssp and Spl) in various growth phases, including biofilm (Fig. 4). Atl is processed collaboratively by the serine protease Ssp and the cysteine protease Spl (Rice *et al.*, 2001). These proteases modulate the activity, stability and translocation of Atl, and affect the autolysis and biofilm development of *S. aureus* (Rice *et al.*, 2001; Biswas *et al.*, 2006; Thomas *et al.*, 2008; Lauderdale *et al.*, 2009; Chen *et al.*, 2013; Grilo *et al.*, 2014).

We conclude that the *msaABCR* operon plays a key role in maintaining the balance between autolysis and growth within a biofilm. The *msaABCR* operon achieves this balance by controlling the expression of the proteases that process the major autolysin, Atl. The environmental signals to which this operon responds are still unknown. Other regulators have been shown to control biofilm development via proteases. For instance, *sarA* mutants are biofilm negative because of their increased production of proteases (Beenken *et al.*, 2010; Zielinska *et al.*, 2012). Similarly, SigB also regulates biofilm formation via an *agr*/protease-dependent pathway (Lauderdale *et al.*, 2009).

We plan to investigate the relationship between *msaABCR* and these global regulators.

SUPPLEMENTARY DATA

Supplementary data is available at FEMSLE online.

ACKNOWLEDGEMENTS

The authors are grateful to Dr Lindsey N. Shaw for sharing *S. aureus* strain USA300 LAC and to Dr Taeok Bae for providing the plasmid pKOR1. We are also grateful to Dr Jeffrey L. Bose and Dr Kenneth W. Bayles for sharing *S. aureus* strain LAC 13C (*atl*) and to Dr Mark S. Smeltzer for the protease mutant LAC strains.

FUNDING

This work was funded by the National Institutes of Health (grant 1R15AI099922, to MOE) and by the Mississippi INBRE, with an Institutional Development Award (IDeA) of the National Institute of General Medical Sciences (grant number P20GM103476).

Conflict of interest statement. None declared.

REFERENCES

Bae T, Schneewind O. Allelic replacement in *Staphylococcus aureus* with inducible counter-selection. *Plasmid* 2006;**55**:58–63.

Bayles KW. The biological role of death and lysis in biofilm development. *Nat Rev Microbiol* 2007;**5**:721–6.

Beenken KE, Blevins JS, Smeltzer MS. Mutation of *sarA* in *Staphylococcus aureus* limits biofilm formation. *Infect Immun* 2003;**71**:4206–11.

Beenken KE, Mrak LN, Griffin LM, *et al.* Epistatic relationships between *sarA* and *agr* in *Staphylococcus aureus* biofilm formation. *PLoS One* 2010;**5**:e10790.

Beenken KE, Spencer H, Griffin LM, *et al.* Impact of extracellular nuclease production on the biofilm phenotype of *Staphylococcus aureus* under in vitro and in vivo conditions. *Infect Immun* 2012;**80**:1634–8.

Biswas R, Voggu L, Simon UK, *et al.* Activity of the major staphylococcal autolysin Atl. *FEMS Microbiol Lett* 2006;**259**:260–8.

Bitoun JP, Liao S, McKey BA, *et al. Psr* is involved in regulation of glucan production, and double deficiency of *BrpA* and *Psr* is lethal in *Streptococcus mutans*. *Microbiology* 2013;**159**:493–506.

Boles BR, Horswill AR. *Agr*-mediated dispersal of *Staphylococcus aureus* biofilms. *PLoS Pathog* 2008;**4**:e1000052.

Boles BR, Thoendel M, Roth AJ, *et al.* Identification of genes involved in polysaccharide-independent *Staphylococcus aureus* biofilm formation. *PLoS One* 2010;**5**:e10146.

Bose JL, Lehman MK, Fey PD, *et al.* Contribution of the *Staphylococcus aureus* Atl AM and GL Murein hydrolase activities in cell division, autolysis, and biofilm formation. *PLoS One* 2012;**7**:e42244.

Chan YG, Frankel MB, Dengler V, *et al. Staphylococcus aureus* mutants lacking the LytR-CpsA-Psr family of enzymes release cell wall teichoic acids into the extracellular medium. *J Bacteriol* 2013;**195**:4650–9.

Charpentier E, Anton AI, Barry P, *et al.* Novel cassette-based shuttle vector system for gram-positive bacteria. *Appl Environ Microb* 2004;**70**:6076–85.

Chen C, Krishnan V, Macon K, *et al.* Secreted proteases control autolysin-mediated biofilm growth of *Staphylococcus aureus*. *J Biol Chem* 2013;**288**:29440–52.

Cramton SE, Gerke C, Schnell NF, *et al.* The intercellular adhesion (*ica*) locus is present in *Staphylococcus aureus* and is required for biofilm formation. *Infect Immun* 1999;**67**:5427–33.

Fitzpatrick F, Humphreys H, O'Gara JP. Evidence for *icaADBC*-independent biofilm development mechanism in methicillin-resistant *Staphylococcus aureus* clinical isolates. *J Clin Microbiol* 2005;**43**:1973–6.

Grilo IR, Ludovice AM, Tomasz A, *et al.* The glucosaminidase domain of Atl — the major *Staphylococcus aureus* autolysin — has DNA-binding activity. *MicrobiologyOpen* 2014;**3**:247–56.

Groicher KH, Firek BA, Fujimoto DF, *et al.* The *Staphylococcus aureus lrgAB* operon modulates murein hydrolase activity and penicillin tolerance. *J Bacteriol* 2000;**182**:1794–801.

Gross M, Cramton SE, Gotz F, *et al.* Key role of teichoic acid net charge in *Staphylococcus aureus* colonization of artificial surfaces. *Infect Immun* 2001;**69**:3423–6.

Haque NZ, Davis SL, Manierski CL, *et al.* Infective endocarditis caused by USA300 methicillin-resistant *Staphylococcus aureus* (MRSA). *Int J Antimicrob Ag* 2007;**30**:72–7.

Heilmann C, Gerke C, Perdreau-Remington F, *et al.* Characterization of Tn917 insertion mutants of *Staphylococcus epidermidis* affected in biofilm formation. *Infect Immun* 1996;**64**:277–82.

Herold BC, Immergluck LC, Maranan MC, *et al.* Community-acquired methicillin-resistant *Staphylococcus aureus* in children with no identified predisposing risk. *Jama* 1998;**279**:593–8.

Heydorn A, Nielsen AT, Hentzer M, *et al.* Quantification of biofilm structures by the novel computer program COMSTAT. *Microbiology* 2000;**146**:2395–407.

Horsburgh MJ, Aish JL, White IJ, *et al. sigmaB* modulates virulence determinant expression and stress resistance: characterization of a functional *rsbU* strain derived from *Staphylococcus aureus* 8325–4. *J Bacteriol* 2002;**184**:5457–67.

Houston P, Rowe SE, Pozzi C, *et al.* Essential role for the major autolysin in the fibronectin-binding protein-mediated *Staphylococcus aureus* biofilm phenotype. *Infect Immun* 2011;**79**:1153–65.

Kiedrowski MR, Kavanaugh JS, Malone CL, *et al.* Nuclease modulates biofilm formation in community-associated methicillin-resistant *Staphylococcus aureus*. *PLoS One* 2011;**6**:e26714.

Kullik I, Giachino P, Fuchs T. Deletion of the alternative sigma factor *sigmaB* in *Staphylococcus aureus* reveals its function as a global regulator of virulence genes. *J Bacteriol* 1998;**180**:4814–20.

Lauderdale KJ, Boles BR, Cheung AL, *et al.* Interconnections between *Sigma B, agr*, and proteolytic activity in *Staphylococcus aureus* biofilm maturation. *Infect Immun* 2009;**77**:1623–35.

Ledala N, Wilkinson BJ, Jayaswal RK. Effects of oxacillin and tetracycline on autolysis, autolysin processing and atl transcription in *Staphylococcus aureus*. *Int J Antimicrob Ag* 2006;**27**:518–24.

Lowy FD. *Staphylococcus aureus* infections. *New Engl J Med* 1998;**339**:520–32.

Mani N, Tobin P, Jayaswal RK. Isolation and characterization of autolysis-defective mutants of *Staphylococcus aureus* created by Tn917-lacZ mutagenesis. *J Bacteriol* 1993;**175**:1493–9.

Mann EE, Rice KC, Boles BR, *et al*. Modulation of eDNA release and degradation affects *Staphylococcus aureus* biofilm maturation. *PLoS One* 2009;**4**:e5822.

Merino N, Toledo-Arana A, Vergara-Irigaray M, *et al*. Protein A-mediated multicellular behavior in *Staphylococcus aureus*. *J Bacteriol* 2009;**191**:832–43.

Mootz JM, Malone CL, Shaw LN, *et al*. Staphopains modulate *Staphylococcus aureus* biofilm integrity. *Infect Immun* 2013;**81**:3227–38.

Oshida T, Sugai M, Komatsuzawa H, *et al*. A *Staphylococcus aureus* autolysin that has an N-acetylmuramoyl-L-alanine amidase domain and an endo-beta-N-acetylglucosaminidase domain: cloning, sequence analysis, and characterization. *P Natl Acad Sci USA* 1995;**92**:285–9.

Otto M. Staphylococcal infections: mechanisms of biofilm maturation and detachment as critical determinants of pathogenicity. *Annu Rev Med* 2013;**64**:175–88.

Perkins HR. The bacterial autolysins. In: Rogers HJ, Perkins HJ, Ward JB (eds). *Microbial Cell Walls* London, UK: Chapman and Hall, 1980, 437–56.

Qamar A, Golemi-Kotra D. Dual roles of FmtA in *Staphylococcus aureus* cell wall biosynthesis and autolysis. *Antimicrob Agents Ch* 2012;**56**:3797–805.

Qin Z, Ou Y, Yang L, *et al*. Role of autolysin-mediated DNA release in biofilm formation of *Staphylococcus epidermidis*. *Microbiology* 2007;**153**:2083–92.

Rice K, Peralta R, Bast D, *et al*. Description of *staphylococcus* serine protease (*ssp*) operon in *Staphylococcus aureus* and nonpolar inactivation of *sspA*-encoded serine protease. *Infect Immun* 2001;**69**:159–69.

Rice KC, Firek BA, Nelson JB, *et al*. The *Staphylococcus aureus cidAB* operon: evaluation of its role in regulation of murein hydrolase activity and penicillin tolerance. *J Bacteriol* 2003;**185**:2635–43.

Rice KC, Mann EE, Endres JL, *et al*. The *cidA* murein hydrolase regulator contributes to DNA release and biofilm development in *Staphylococcus aureus*. *P Natl Acad Sci USA* 2007;**104**:8113–8.

Sahukhal GS, Elasri MO. Identification and characterization of an operon, *msaABCR*, that controls virulence and biofilm development in *Staphylococcus aureus*. *BMC Microbiol* 2014;**14**:154.

Sambanthamoorthy K, Schwartz A, Nagarajan V, *et al*. The Role of *msa* in *Staphylococcus aureus* Biofilm Formation. *BMC Microbiol* 2008;**8**:221.

Sambanthamoorthy K, Smeltzer MS, Elasri MO. Identification and characterization of *msa* (SA1233), a gene involved in expression of *SarA* and several virulence factors in *Staphylococcus aureus*. *Microbiology* 2006;**152**:2559–72.

Thomas VC, Thurlow LR, Boyle D, *et al*. Regulation of autolysis-dependent extracellular DNA release by *Enterococcus faecalis* extracellular proteases influences biofilm development. *J Bacteriol* 2008;**190**:5690–8.

Toledo-Arana A, Merino N, Vergara-Irigaray M, *et al*. *Staphylococcus aureus* develops an alternative, ica-independent biofilm in the absence of the *arlRS* two-component system. *J Bacteriol* 2005;**187**:5318–29.

Tsang LH, Cassat JE, Shaw LN, *et al*. Factors contributing to the biofilm-deficient phenotype of *Staphylococcus aureus sarA* mutants. *PLoS One* 2008;**3**:e3361.

Wadstrom T, Hisatsune K. Bacteriolytic enzymes from *Staphylococcus aureus*. Specificity of ction of endo-beta-N-acetylglucosaminidase. *Biochem J* 1970;**120**:735–44.

Wang X, Mani N, Pattee PA, *et al*. Analysis of a peptidoglycan hydrolase gene from *Staphylococcus aureus* NCTC 8325. *J Bacteriol* 1992;**174**:6303–6.

Wen ZT, Baker HV, Burne RA. Influence of *BrpA* on critical virulence attributes of *Streptococcus mutans*. *J Bacteriol* 2006;**188**:2983–92.

Whitchurch CB, Tolker-Nielsen T, Ragas PC, *et al*. Extracellular DNA required for bacterial biofilm formation. *Science* 2002;**295**:1487.

Zielinska AK, Beenken KE, Mrak LN, *et al*. *sarA*-mediated repression of protease production plays a key role in the pathogenesis of *Staphylococcus aureus* USA300 isolates. *Mol Microbiol* 2012;**86**:1183–96.